

# Thermoelectric Properties of Ca-Filled CoSb<sub>3</sub>-Based Skutterudites Synthesized by Mechanical Alloying

KWAN-HO PARK<sup>1</sup> and IL-HO KIM<sup>1,2</sup>

1.—Department of Materials Science and Engineering, Chungju National University, 50 Daehangno, Chungbuk 380-702, Korea. 2.—e-mail: ihkim@cjnu.ac.kr

Ca<sub>z</sub>Co<sub>4-x</sub>(Fe/Mn)<sub>x</sub>Sb<sub>12</sub> skutterudites were prepared by mechanical alloying and hot pressing. The phases of mechanically alloyed powders were identified as  $\gamma$ -CoSb<sub>2</sub> and Sb, but they were transformed to  $\delta$ -CoSb<sub>3</sub> by annealing at 873 K for 100 h. All specimens had a positive Hall coefficient and Seebeck coefficient, indicating *p*-type conduction by holes as majority carriers. For the binary CoSb<sub>3</sub>, the electrical conductivity behaved like a nondegenerate semiconductor, but Ca-filled and Fe/Mn-doped CoSb<sub>3</sub> showed a temperature dependence of a degenerate semiconductor. While the Seebeck coefficient of intrinsic CoSb<sub>3</sub> increased with temperature and reached a maximum at 623 K, the Seebeck coefficient increased with increasing temperature for the Ca-filled and Fe/Mn-doped specimens. Relatively low thermal conductivity was obtained because fine particles prepared by mechanical alloying lead to phonon scattering. The thermal conductivity was reduced by Ca filling and Fe/Mn doping. The electronic thermal conductivity was increased by Fe/Mn doping, but the lattice thermal conductivity was decreased by Ca filling. Reasonable thermoelectric figure-of-merit values were obtained for Ca-filled Co-rich *p*-type skutterudites.

**Key words:** Thermoelectric, skutterudite, CoSb<sub>3</sub>, mechanical alloying

## INTRODUCTION

The skutterudite structure consists of 8TX<sub>3</sub> in the unit cell, where T represents a transition atom (Co, Rh, Ir) and X a pnictogen atom (P, As, Sb). It was discovered that intrinsic CoSb<sub>3</sub> has a bandgap energy of 0.5 eV and its conduction band is very flat, implying a larger electron effective mass and the potential for excellent thermoelectric properties.<sup>1</sup> CoSb<sub>3</sub>-based skutterudites are promising thermoelectric materials but have low figures of merit due to the high thermal conductivity. Filled skutterudites are compounds in which the Sb icosahedron voids in the crystal structure are filled with metal atoms. Filling atoms with small ionic radius have weak binding force to adjacent atoms and “rattle” markedly in the oversized cages, which causes intensive scattering of phonons, so that the lattice

thermal conductivity can be reduced significantly.<sup>2–5</sup> Substitution of Co or Sb by dopants can affect the electronic structure and electrical properties, and cause a substantial change in carrier mass. Furthermore, doping can also affect the lattice thermal conductivity due to phonon scattering on impurities.<sup>6</sup> Therefore, thermoelectric properties can be optimized by filling of the voids and/or by substitution at the Co or Sb sites. In this context, tremendous efforts have been made with the CoSb<sub>3</sub> skutterudite, and numerous atoms have been used for filling and/or substitution.<sup>7–14</sup>

The research results on filled skutterudites<sup>15–21</sup> indicate that, when rare-earth atoms (e.g., La, Ce, and Yb) with high valence and smaller ionic radius are used as filling atoms, the thermal conductivity of skutterudites can be reduced remarkably, and when alkaline-earth atoms (e.g., Ca, Sr, and Ba) with low valence are used as filling atoms, the skutterudites possess preferable electric transport properties. Some researchers have reported the

(Received May 5, 2010; accepted October 11, 2010; published online November 6, 2010)

structural, electrical, and thermal transport properties of  $\text{CoSb}_3$  partially filled with Ca, prepared using melting or solid-state reaction methods.<sup>22,23</sup> They suggested that the thermoelectric properties could be enhanced considerably by Ca filling. Dudkin<sup>24</sup> reported a doping study of  $\text{CoSb}_3$  in which the effect of 13 different impurity elements on the electronic transport properties was studied.<sup>29</sup> Fe and Ni substituted for Co, and Te substituted for Sb were found to be active dopants, with Ni and Te acting as donors and Fe as an acceptor. Many researchers have reported the thermoelectric properties of  $n$ -type  $\text{CoSb}_3$  doped with different impurities.<sup>1,3,6,25,26</sup> However, there are few studies concerning  $p$ -type  $\text{CoSb}_3$ ,<sup>27,28</sup> and the effect of doping on the transport and thermoelectric properties is still an important subject to be examined. In this study, Ca-filled and Fe/Mn-doped  $\text{CoSb}_3$  skutterudites were prepared by mechanical alloying and hot pressing. The effects of filling and doping on the thermoelectric and transport properties were examined.

## EXPERIMENTAL PROCEDURES

Ca-filled skutterudites  $\text{Ca}_z\text{Co}_{4-x}(\text{Fe/Mn})_x\text{Sb}_{12}$  ( $z = 0, 0.3$ ;  $x = 1.0, 1.5$ ) were synthesized by mechanical alloying (MA). Elemental powders of Ca (purity 99.5%), Co (purity 99.95%), Fe (purity 99.9%), Mn (purity 99.9%), and Sb (purity 99.9%) were loaded into a hardened-steel vial in argon atmosphere with hardened-steel balls (diameter 5 mm) at a weight ratio of 1:20. The vial was then loaded into a planetary ball mill (Fritsch, Pulverisette 5) and subjected to MA at 300 rpm for 48 h. The mechanically alloyed powders were cold-pressed under a pressure of 600 MPa to make pellets, which were annealed in an evacuated quartz ampoule at 873 K for 100 h to homogenize the sample and to allow sufficient time for Ca to fill the voids in the skutterudite structure as well as for Fe/Mn dopant activation. The pellet was ground to powder and sieved to a particle size of 45  $\mu\text{m}$ . These synthesized powders were hot-pressed in a cylindrical hardened-steel die with an internal diameter of 10 mm at 873 K under a pressure of 70 MPa for 2 h in a vacuum. The hot-pressed samples had nearly full density (higher than 98%).

The hot-pressed compact with dimensions of 10 mm (diameter)  $\times$  10 mm (length) was cut to a rectangular-shaped piece with dimensions of 3 mm  $\times$  3 mm  $\times$  9 mm for both Seebeck coefficient and electrical conductivity measurements, and cut to a disc-shaped piece with dimensions of 10 mm (diameter)  $\times$  1 mm (thickness) for both thermal conductivity and Hall-effect measurements. A scanning electron microscope (SEM; FEI Quanta400) equipped with an energy-dispersive spectrometer (EDS; Oxford JSM-5800) was used to observe the microstructure. Phase analysis was performed by an x-ray diffractometer (XRD; Bruker

D8 Advance) using  $\text{Cu K}_\alpha$  radiation (40 kV, 40 mA). Diffraction patterns were measured in  $\theta$ - $2\theta$  mode (10–90°) with a step size of 0.02°, scan speed of 0.2°/min, and wavelength of 0.15405 nm. Hall-effect measurements (Keithley 7065) were carried out in a constant magnetic field (1 T) and electric current (50 mA) at 300 K. The Seebeck coefficient ( $\alpha$ ), electrical conductivity ( $\sigma$ ), and thermal conductivity ( $\kappa$ ) were measured from 323 K to 823 K, and the dimensionless thermoelectric figure of merit ( $ZT = \alpha^2\sigma T\kappa^{-1}$ ) was evaluated, where  $T$  is temperature in Kelvin. The Seebeck coefficient and electrical resistivity were measured using temperature differential and four-probe methods (Ulvac-Riko ZEM2-M8), respectively. The thermal conductivity was evaluated by measuring the thermal diffusivity, specific heat, and density using the laser flash method (Ulvac-Riko TC7000).

## RESULTS AND DISCUSSION

Figure 1 shows the x-ray diffraction patterns of the  $\text{Ca}_z\text{Co}_{4-x}(\text{Fe or Mn})_x\text{Sb}_{12}$  skutterudites. Very broad diffraction peaks were observed for mechanically alloyed powders due to fine particles with residual stress produced during MA. The phases were identified as  $\gamma$ - $\text{CoSb}_2$  and Sb, but subsequent annealing at 873 K for 100 h and hot pressing resulted in full transformation to  $\delta$ - $\text{CoSb}_3$  with sharp diffraction peaks. However, as shown in Fig. 1d and f, it decomposed to  $\text{FeSb}_2$  (or  $\text{MnSb}$ ) and Sb when  $x = 1.5$ . A similar result has been reported in hot-pressed  $\text{Co}_{1-x}\text{Fe}_x\text{Sb}_3$ ,<sup>27,28</sup> being related to the solubility limit of Fe to Co. Although the secondary phase  $\text{FeSb}_2$  for  $\text{CoSb}_3$ -based skutterudites has been reported, the secondary phase  $\text{MnSb}$  has not been reported yet. In this study, Mn showed a similar behavior to Fe in  $\text{CoSb}_3$ -based skutterudites.

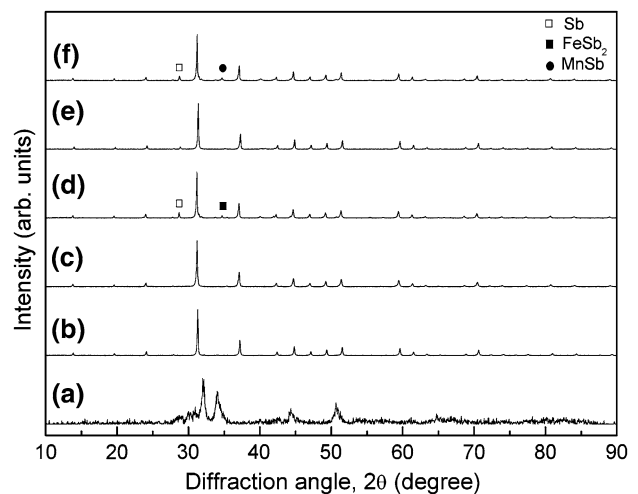


Fig. 1. X-ray diffraction patterns of the  $\text{Ca}_z\text{Co}_{4-x}(\text{Fe/Mn})_x\text{Sb}_{12}$  skutterudites prepared by mechanical alloying (MA) and hot pressing (HP): (a) mechanically alloyed  $\text{Co}_4\text{Sb}_{12}$  powders, (b) hot-pressed  $\text{Co}_4\text{Sb}_{12}$ , (c)  $\text{Ca}_{0.3}\text{Co}_3\text{FeSb}_{12}$ , (d)  $\text{Ca}_{0.3}\text{Co}_{2.5}\text{Fe}_{1.5}\text{Sb}_{12}$ , (e)  $\text{Ca}_{0.3}\text{Co}_3\text{MnSb}_{12}$ , and (f)  $\text{Ca}_{0.3}\text{Co}_{2.5}\text{Mn}_{1.5}\text{Sb}_{12}$ .

**Table I. Transport properties and lattice constant of Ca<sub>2</sub>Co<sub>4-x</sub>(Fe/Mn)<sub>x</sub>Sb<sub>12</sub> at 300 K**

Nominal Composition	Hall Coeff. (cm <sup>3</sup> /C)	Mobility (cm <sup>2</sup> /Vs)	Carrier Conc. (cm <sup>-3</sup> )	Lattice Constant (nm)
Co <sub>4</sub> Sb <sub>12</sub>	$4.32 \times 10^{-1}$	39.85	$1.46 \times 10^{20}$	0.90346
Ca <sub>0.3</sub> Co <sub>3</sub> FeSb <sub>12</sub>	$2.93 \times 10^{-2}$	24.55	$2.14 \times 10^{20}$	0.90572
Ca <sub>0.3</sub> Co <sub>2.5</sub> Fe <sub>1.5</sub> Sb <sub>12</sub>	$2.35 \times 10^{-2}$	25.50	$2.66 \times 10^{20}$	0.90650
Ca <sub>0.3</sub> Co <sub>3</sub> MnSb <sub>12</sub>	$3.35 \times 10^{-2}$	28.62	$1.97 \times 10^{20}$	0.90568
Ca <sub>0.3</sub> Co <sub>2.5</sub> Mn <sub>1.5</sub> Sb <sub>12</sub>	$2.46 \times 10^{-2}$	27.86	$2.63 \times 10^{20}$	0.90587

Table I presents the lattice constant together with the electronic transport properties of Ca<sub>2</sub>Co<sub>4-x</sub>(Fe/Mn)<sub>x</sub>Sb<sub>12</sub>. The lattice constant of intrinsic CoSb<sub>3</sub> was 0.90346 nm, increasing to 0.90568 nm to 0.90650 nm by Ca filling and Fe/Mn doping. The Hall coefficient, carrier mobility, and carrier concentration were examined for Ca<sub>2</sub>Co<sub>4-x</sub>(Fe/Mn)<sub>x</sub>Sb<sub>12</sub> at 300 K. Intrinsic CoSb<sub>3</sub> shows a positive Hall coefficient (*p*-type conduction), because its hole mobility is much higher than its electron mobility; i.e., the effective hole mass is much smaller than the effective electron mass. The achievement of *p*-type conduction is in good agreement with the results reported by Nolas et al.<sup>5</sup> and Sharp et al.<sup>29</sup> on polycrystalline CoSb<sub>3</sub>. However, it is different from those of Morelli et al.<sup>4</sup> and Kuznetsov et al.,<sup>12</sup> who obtained *n*-type conduction at room temperature. The origin of these discrepancies regarding *n*- or *p*-type conduction in CoSb<sub>3</sub> skutterudites has been discussed by several authors. According to Morelli et al.<sup>4</sup> the *p*- (*n*-)type behavior would be due to a lack of cobalt (antimony), respectively. It is, however, now well established that the purity of the raw cobalt material plays an essential role in the electrical properties found in CoSb<sub>3</sub>.<sup>30,31</sup> The use of cobalt free of residual nickel impurity leads to positive conduction. Some hundreds of ppm of residual nickel impurity in cobalt are enough to switch the material from *p*- to *n*-type conduction.

Puyet et al.<sup>23</sup> reported that the introduction of Ca into the voids of the skutterudite structure has a strong effect on the thermoelectric properties and that Ca filling in Ca<sub>2</sub>Co<sub>4</sub>Sb<sub>12</sub> leads to a negative Hall coefficient, while it is positive for the CoSb<sub>3</sub> binary skutterudite. In this study, all Ca<sub>2</sub>Co<sub>4-x</sub>(Fe/Mn)<sub>x</sub>Sb<sub>12</sub> specimens had a positive Hall coefficient, which means that Ca-filled and Fe/Mn-doped CoSb<sub>3</sub> shows *p*-type conduction by holes as majority carriers. Fe/Mn doping could signify a higher density of hole-like charge carriers than that of electron-like charge carriers due to Ca filling in CoSb<sub>3</sub>. The hole concentration was increased from the order of 10<sup>19</sup> cm<sup>-3</sup> to 10<sup>20</sup> cm<sup>-3</sup> by Fe/Mn doping.

Figure 2 illustrates the microstructure of Ca<sub>2</sub>Co<sub>4-x</sub>(Fe/Mn)<sub>x</sub>Sb<sub>12</sub> prepared by mechanical alloying and hot pressing. The mean particle size of mechanically alloyed powders was a few microns, and the particle shape was irregular. A very solid and compact microstructure with few pores and cracks could be obtained by hot pressing.

Homogeneous specimens were achieved, but the secondary phases (FeSb<sub>2</sub> and MnSb) were observed for Ca<sub>0.3</sub>Co<sub>2.5</sub>(Fe or Mn)<sub>1.5</sub>Sb<sub>12</sub> specimens. This is in good agreement with the XRD analysis results.

Figure 3 shows the temperature dependence of the electrical conductivity ( $\sigma$ ) of Ca<sub>2</sub>Co<sub>4-x</sub>(Fe/Mn)<sub>x</sub>Sb<sub>12</sub>. For the binary CoSb<sub>3</sub>, the electrical conductivity was as low as high 10<sup>3</sup> S/m, but it gradually increased with increasing temperature, which implies the possibility of intrinsic behavior at high temperatures. The electrical conductivity decreased slightly with increasing temperature, which is mainly due to the effect of scattering of the carriers by the crystal lattice being enhanced with increasing temperature. Ca-filled and Fe/Mn-doped CoSb<sub>3</sub> was found to be a degenerate semiconductor, and the electrical conductivity ranged from the order of high 10<sup>4</sup> S/m to low 10<sup>5</sup> S/m. The electrical conductivity increased with increasing Fe/Mn doping content due to an increase in carrier concentration.

Figure 4 presents the temperature dependence of the Seebeck coefficient ( $\alpha$ ) of Ca<sub>2</sub>Co<sub>4-x</sub>(Fe/Mn)<sub>x</sub>Sb<sub>12</sub>. All specimens had a positive Seebeck coefficient, which confirms the Hall coefficient in Table I. While the Seebeck coefficient of intrinsic CoSb<sub>3</sub> increased with temperature and reached a maximum at 623 K, the Seebeck coefficient increased with increasing temperature for the Ca-filled and Fe/Mn-doped specimens. However, the slope decreased with increasing Fe/Mn doping content. This is related to an increase in hole concentration by Fe/Mn doping. In general, the Seebeck coefficient decreases with increasing carrier concentration. The Seebeck coefficient of Ca<sub>0.3</sub>Co<sub>3</sub>(Fe or Mn)Sb<sub>12</sub> was obtained as 125  $\mu$ V/K at 823 K, similar to the value of 120  $\mu$ V/K at 800 K in the Ca<sub>0.45</sub>Co<sub>2.4</sub>Fe<sub>1.6</sub>Sb<sub>12</sub> reported by Tang et al.<sup>22</sup>

Figure 5 shows the temperature dependence of the thermal conductivity ( $\kappa$ ) of Ca<sub>2</sub>Co<sub>4-x</sub>(Fe/Mn)<sub>x</sub>Sb<sub>12</sub>. The thermal conductivity was evaluated by measuring the thermal diffusivity ( $D$ ), specific heat ( $C_p$ ), and density ( $d$ ) using the relation  $\kappa = dC_p D$ . Malik et al.<sup>32</sup> reported on the intrinsic CoSb<sub>3</sub> prepared by induction melting in an evacuated quartz ampoule. Intrinsic CoSb<sub>3</sub> has a much higher thermal conductivity, being 11 W/mK at 300 K and decreasing with increasing temperature to 7.4 W/mK at 700 K. In this study, however, a relatively low thermal conductivity of 2.5 W/mK to 3.9 W/mK was obtained because fine particles

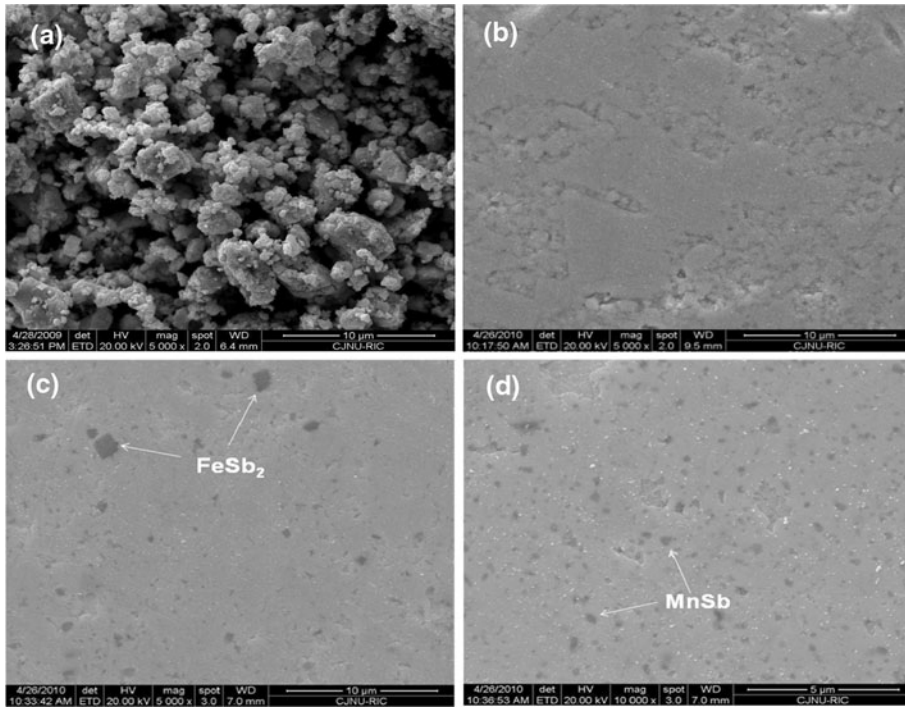


Fig. 2. Scanning electron microscope images of the  $\text{Ca}_2\text{Co}_{4-x}(\text{Fe/Mn})_x\text{Sb}_{12}$  skutterudites prepared by mechanical alloying (MA) and hot pressing (HP): (a) mechanically alloyed  $\text{Co}_4\text{Sb}_{12}$  powders, (b) hot-pressed  $\text{Co}_4\text{Sb}_{12}$ , (c)  $\text{Ca}_{0.3}\text{Co}_{2.5}\text{Fe}_{1.5}\text{Sb}_{12}$ , (d)  $\text{Ca}_{0.3}\text{Co}_{2.5}\text{Mn}_{1.5}\text{Sb}_{12}$ .

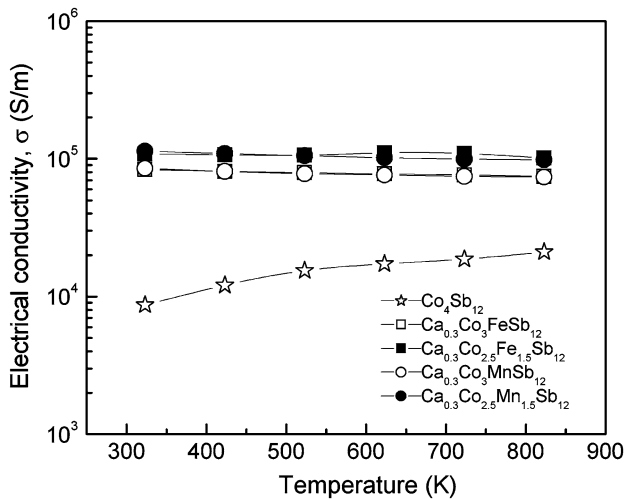


Fig. 3. Temperature dependence of the electrical conductivity of  $\text{Ca}_2\text{Co}_{4-x}(\text{Fe/Mn})_x\text{Sb}_{12}$ .

prepared by mechanical alloying lead to phonon scattering. The thermal conductivity was reduced by Ca filling and Fe/Mn doping. The thermal conductivity ( $\kappa = \kappa_L + \kappa_E$ ) was separated into the lattice thermal conductivity ( $\kappa_L$ ) and electronic thermal conductivity ( $\kappa_E$ ) using the Wiedemann–Franz law ( $\kappa_E = L\sigma T$ ), where the Lorenz number was assumed to be a constant ( $L = 2.45 \times 10^{-8} \text{ V}^2/\text{K}^2$ ) for the evaluation.<sup>33</sup> Figure 5b and c shows the separation of the electronic contribution and the lattice contribution to the thermal conductivity. The electronic

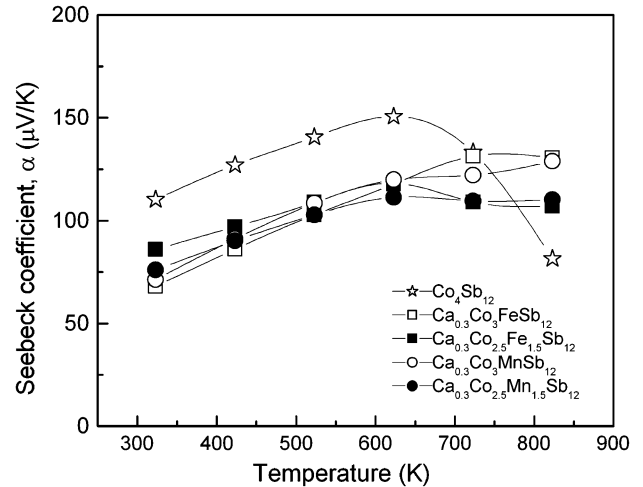


Fig. 4. Temperature dependence of the Seebeck coefficient of  $\text{Ca}_2\text{Co}_{4-x}(\text{Fe/Mn})_x\text{Sb}_{12}$ .

thermal conductivity was increased by Fe/Mn doping, and it increased more when the doping content was larger. Ca filling reduced the lattice thermal conductivity due to the rattling effect.

Figure 6 indicates the temperature dependence of the dimensionless figure of merit ( $ZT$ ) of  $\text{Ca}_2\text{Co}_{4-x}(\text{Fe/Mn})_x\text{Sb}_{12}$ . The  $ZT$  value increased rapidly with increasing temperature, mainly due to an increase in the Seebeck coefficient and the maintenance of low thermal conductivity at high temperatures. The secondary phases ( $\text{FeSb}_2$  and



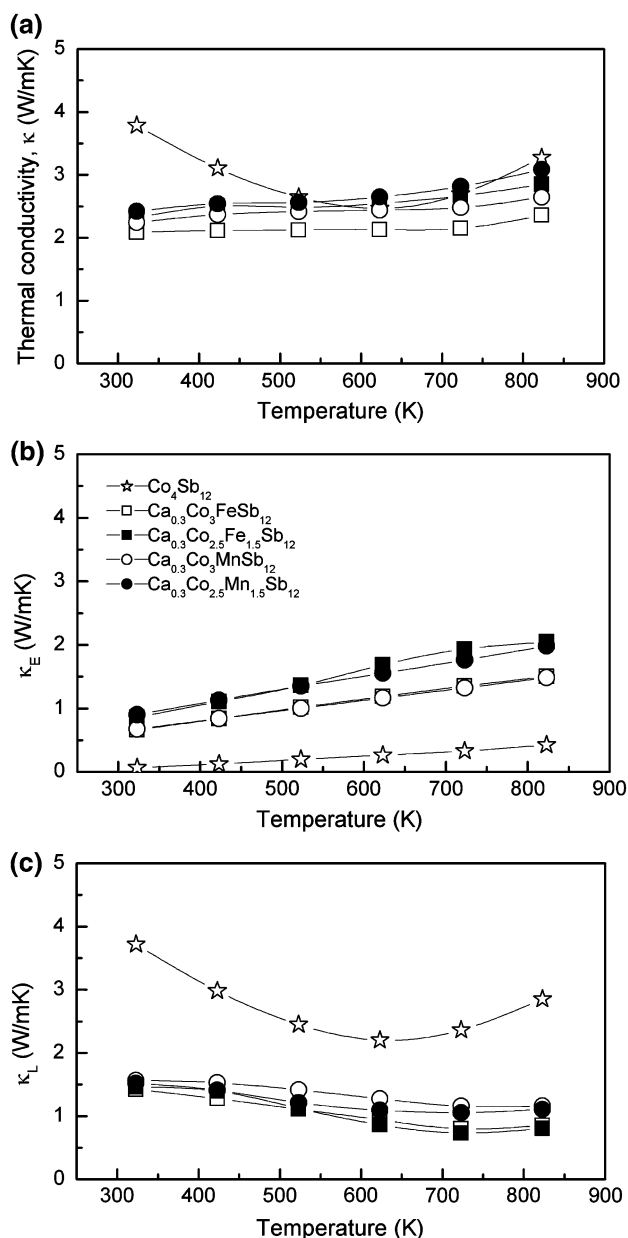


Fig. 5. Temperature dependence of the thermal conductivity of Ca<sub>2</sub>Co<sub>4-x</sub>(Fe/Mn)<sub>x</sub>Sb<sub>12</sub>: (a) total thermal conductivity, (b) electronic thermal conductivity, and (c) lattice thermal conductivity.

MnSb) had a negative effect on the thermoelectric properties for Ca<sub>2</sub>Co<sub>4-x</sub>(Fe/Mn)<sub>x</sub>Sb<sub>12</sub> at high temperatures, even though they increased the electrical conductivity. A maximum ZT of 0.44 at 723 K to 823 K was obtained for the Ca<sub>0.3</sub>Co<sub>3</sub>FeSb<sub>12</sub> specimen and 0.39 at 823 K for the Ca<sub>0.3</sub>Co<sub>3</sub>MnSb<sub>12</sub> specimen, which are reasonable values for Ca-filled Co-rich *p*-type skutterudites.

## CONCLUSIONS

Ca-filled and Fe/Mn-doped skutterudites Ca<sub>2</sub>Co<sub>4-x</sub>(Fe/Mn)<sub>x</sub>Sb<sub>12</sub> were synthesized by mechanical alloying and consolidated by hot pressing.

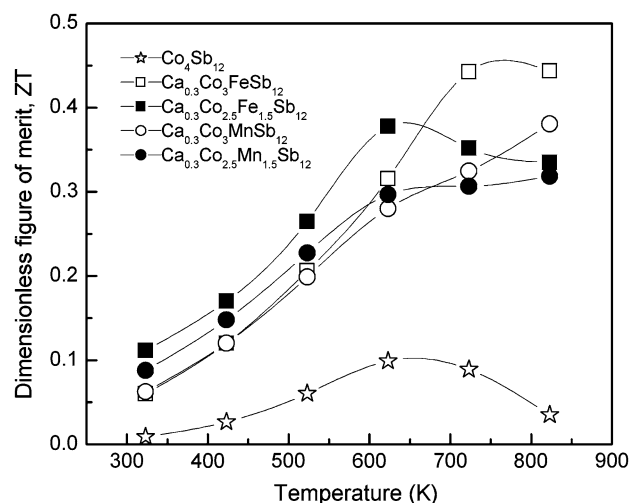


Fig. 6. The dimensionless figure of merit of Ca<sub>2</sub>Co<sub>4-x</sub>(Fe/Mn)<sub>x</sub>Sb<sub>12</sub>.

Subsequent annealing after mechanical alloying could transform to the  $\delta$ -CoSb<sub>3</sub> phase, but secondary phases such as FeSb<sub>2</sub> and MnSb were found when the doping content  $x = 1.5$ . The positive signs of the Seebeck coefficients for all specimens revealed that Fe/Mn atoms acted as *p*-type dopants by substituting Co atoms. The electrical conductivity increased with increasing Fe and Mn doping content due to the increase in carrier concentration, and its temperature dependence indicated degenerate behavior. For the same doping content  $x$ , Mn-doped specimens had similar electrical conductivities to Fe-doped specimens. The Seebeck coefficient increased with increasing temperature for the Ca-filled and Fe/Mn-doped specimens, while the Seebeck coefficient of intrinsic CoSb<sub>3</sub> increased with temperature and reached a maximum at a certain temperature. Ca filling affected the decrease in the thermal conductivity because the lattice thermal conductivity was reduced drastically by Ca filling, although the electronic thermal conductivity was increased by Fe/Mn doping. The ZT increased rapidly with increasing temperature, and a maximum ZT of 0.44 at 723 K to 823 K for Ca<sub>0.3</sub>Co<sub>3</sub>FeSb<sub>12</sub> and 0.39 at 823 K for Ca<sub>0.3</sub>Co<sub>3</sub>MnSb<sub>12</sub> were obtained.

## ACKNOWLEDGEMENTS

This work was supported by the Energy Efficiency & Resources of the Korea Institute of Energy Technology Evaluation and Planning (KETEP) grant funded by the Ministry of Knowledge Economy, Republic of Korea (2008EID11P0630202009) and by the Regional Innovation Center (RIC) Program funded by the Ministry of Knowledge Economy, Republic of Korea.

## REFERENCES

1. T. Caillat, A. Borshchovsky, and J.-P. Fleurial, *Proceedings of the 13th International Conference on Thermoelectrics* (1994), p. 58.

2. B.C. Sales, D. Mandrus, B.C. Chakoumakos, V. Keppens, and J.R. Thomson, *Phys. Rev. B* 56, 15081 (1997).
3. T. Caillat, A. Borshevsky, and J.P. Fleurial, *J. Appl. Phys.* 80, 4442 (1996).
4. D.T. Morelli, G.P. Meisner, B.X. Chen, S.Q. Hu, and C. Uher, *Phys. Rev. B* 56, 7376 (1997).
5. G.S. Nolas, J.L. Cohn, and G.A. Slack, *Phys. Rev. B* 58, 164 (1998).
6. K.T. Wojciechowski, J. Tobol, and J. Leszczynski, *J. Alloys Compd.* 361, 19 (2003).
7. N.R. Dilley, E.D. Bauer, M.B. Maple, and B.C. Sales, *J. Appl. Phys.* 88, 1948 (2000).
8. B.C. Sales, B.C. Chakoumakos, and D. Mandrus, *Phys. Rev. B* 61, 2475 (2000).
9. G.S. Nolas, H. Takizawa, T. Endo, H. Sellin, and D.C. Johnson, *Appl. Phys. Lett.* 77, 52 (2000).
10. J.S. Dyck, W. Chen, C. Uher, L. Chen, X. Tang, and T. Hirai, *J. Appl. Phys.* 91, 3698 (2002).
11. J. Yang, D.T. Morelli, G.P. Meisner, W. Chen, J.S. Dyck, and C. Uher, *Phys. Rev. B* 67, 165207 (2003).
12. V.L. Kuznetsov, L.A. Kuznetsova, and D.M. Rowe, *J. Phys.: Condens. Matter* 15, 5035 (2003).
13. G.S. Nolas, J. Yang, and H. Takizawa, *Appl. Phys. Lett.* 84, 5210 (2004).
14. M. Puyet, A. Dauscher, B. Lenoir, M. Dehmas, C. Stiewe, E. Müller, and J. Hejtmanek, *J. Appl. Phys.* 97, 083712 (2005).
15. M. Puyet, B. Lenoir, A. Dauscher, M. Dehmas, C. Stiewe, and E. Müller, *J. Appl. Phys.* 95, 4852 (2004).
16. H. Sato, Y. Aoki, T. Namiki, T.D. Matsuda, K. Abe, S. Osaki, S.R. Saha, and H. Sugawara, *Physica B* 328, 34 (2003).
17. G.A. Lamberton Jr., R.H. Tedstrom, T.M. Tritt, and G.S. Nolas, *J. Appl. Phys.* 97, 113715 (2005).
18. D. Cao, F. Bridges, P. Chesler, S. Bushart, E.D. Bauer, and M.B. Maple, *Phys. Rev. B* 70, 094109 (2004).
19. J.L. Feldman, D.J. Singh, C. Kendziora, D. Mandrus, and B.C. Sales, *Phys. Rev. B* 68, 094301 (2003).
20. L.D. Chen, T. Kawahara, X.F. Tang, T. Goto, T. Hirai, J.S. Dyck, W. Chen, and C. Uher, *J. Appl. Phys.* 90, 1864 (2001).
21. X.F. Tang, Q.J. Zhang, L.D. Chen, T. Goto, and T. Hirai, *J. Appl. Phys.* 97, 093712 (2005).
22. X. Tang, H. Li, and Q. Zhang, *J. Appl. Phys.* 100, 123702 (2006).
23. M. Puyet, B. Lenoir, A. Dauscher, and P. Pêcheur, *Phys. Rev. B* 73, 035126 (2006).
24. L.D. Dudkin and N.K. Abrikosov, *Sov. Phys. Sol. Stat.* 1, 126 (1959).
25. K.T. Wojciechowski, *Mater. Res. Bull.* 37, 2023 (2002).
26. H. Anno, K. Matsubara, Y. Notohara, T. Sakakibara, and H. Tashiro, *J. Appl. Phys.* 86, 3780 (1999).
27. S. Katsuyama, Y. Shichijo, M. Ito, K. Majima, and H. Nagai, *J. Appl. Phys.* 84, 6708 (1998).
28. S. Katsuyama, M. Watanabe, M. Kuroki, T. Maehata, and M. Ito, *J. Appl. Phys.* 93, 2758 (2003).
29. J.W. Sharp, E.C. Jones, R.K. Williams, P.M. Martin, and B.C. Sales, *J. Appl. Phys.* 78, 1013 (1995).
30. L.D. Chen, T. Kawahara, X.F. Tang, T. Goto, T. Hirai, J.S. Dyck, W. Chen, and C. Uher, *Proceedings of the 19th International Conference of Thermoelectrics* (2000), p. 348.
31. K. Matsubara, T. Sakakibara, Y. Notohara, H. Anno, H. Shimizu, and T. Koyanagi, *Proceeding of the 15th International Conference on Thermoelectrics* (1996), p. 96.
32. R.C. Mallik, J.-Y. Jung, V.D. Das, S.-C. Ur, and I.-H. Kim, *Solid State Commun.* 141, 233 (2007).
33. C. Kittel, *Introduction to Solid State Physics*, 6th ed. (John Wiley & Sons, Inc., 1986), p. 152.